

Double photoionization of magnesium from threshold to 54 eV photon energy

R. Wehlitz* and P. N. Juranić†

Synchrotron Radiation Center, University of Wisconsin-Madison, Stoughton, Wisconsin 53589, USA

D. V. Lukić

Institute of Physics, 11001 Belgrade, Serbia

(Received 30 July 2008; published 24 September 2008)

We have measured the relative single and double photoionization cross section of magnesium from 22 to 54 eV photon energy using monochromatized synchrotron radiation. The corresponding double-to-single ionization ratio as well as the relative single photoionization cross section compares reasonably well with recent theoretical calculations [A.S. Kheifets and I. Bray, *Phys. Rev. A* **75**, 042703 (2007)]. The photon energy dependence of the ratio can be modeled by a suitably scaled helium double-to-single photoionization ratio. However, to our surprise, a previously proposed scaling model for that ratio does not work in the case of Mg. From the near-threshold double-photoionization cross section we estimate the range of validity of the Wannier threshold law to be about 0.7 eV with a rather small cross section near threshold.

DOI: [10.1103/PhysRevA.78.033428](https://doi.org/10.1103/PhysRevA.78.033428)

PACS number(s): 32.80.Fb

I. INTRODUCTION

Direct double photoionization of atoms in which two electrons are simultaneously emitted is of high interest for understanding electron correlations. Many investigations of double photoionization have focused on helium—the textbook example for double ionization with its two electrons—and were performed using highly sophisticated experimental apparatuses [1]. Double-photoionization experiments on atoms beyond He are still sparse and often less sophisticated due to the difficult handling of the target atom. Theoretical calculations also concentrated first on He, and after achieving satisfactory agreement with experiment [2], the theory moved forward to slightly more complex atoms. Of particular interest are the alkaline-earth metals that are heliumlike atoms insofar as they only have two outer-valence electrons while the other electrons can be approximated as spectators [3]. For a brief overview we mention some of the double-photoionization experiments with alkaline-earth metals below.

Experiments measuring the direct [4–6] and resonant [7,8] double photoionization of beryllium have detected singly and doubly charged photoions at different photon energies. *R*-matrix calculations for the double photoionization of Be were performed around the *K*-edge [9] and fully differential cross sections were calculated over a large energy range using a frozen-core approximation [10]. More calculations followed using a time-dependent close-coupling method [11,12] and a hyperspherical *R*-matrix method [13]. Kazansky and Ostrovsky [14] theoretically studied the near-threshold triple differential cross section for direct double photoionization of alkaline-earth metals from Be to Sr using an extended Wannier ridge model.

Double photoionization of calcium attracted experimental interest and scientists have measured the partial ion yield as

a function of photon energy [15] and detected both electrons in coincidence after resonant [16] and nonresonant [17] double photoionization with the latter experiment being performed at a single photon energy. The coincidence experiments were analyzed theoretically by Maulbetsch *et al.* [18] and Malegat *et al.* [19]. Electron coincidence experiments similar to those for calcium have also been performed for strontium [20,21].

The photoion yield of doubly charged barium ions was measured at lower (20–35 eV) [22,23] and higher photon energies (90–210 eV) [24]. Results from a single experiment concerned with the double-to-single photoionization ratio of Mg have not been published but are presented as a private communication in Ref. [3]. We note here that those ratios are about a factor of 5 higher than theory.

The double-photoionization process of other than alkaline-earth atoms has been investigated as well but, with the exception of Li, only a few experiments and calculations have been performed. Besides a general lack of Mg double-photoionization data, the near-threshold region is of particular interest because the two double-ionized electrons are highly correlated and should behave according to either Wannier's threshold law [25] or Temkin's Coulomb-dipole (CD) theory for double photoionization [26].

Furthermore, in previous double-photoionization studies of beryllium [4] and of lithium [27] a scaling model for the double-to-single photoionization ratio of He, Li, Be, and possibly molecular hydrogen [28] has been found. At the time, it was hoped that this scaling model would allow us to predict the double-to-single photoionization ratios for other elements. However, it has only been tested for five elements so far. Therefore we became interested in measuring the valence double photoionization cross section and double-to-single photoionization ratio of Mg from threshold to below the first $2p \rightarrow n\ell$ inner-shell resonances.

II. EXPERIMENT

The experiment was performed on two normal-incidence monochromator beamlines, namely the Wadsworth beamline

*wehlitz@src.wisc.edu

†Present address: HASYLAB at DESY, Notkestrasse 85, 22607 Hamburg, Germany.

[29] and the U1-NIM beamline [30], and on a plane-grating monochromator (U3-PGM) beamline [31]. All three beamlines are equipped with an undulator photon source located at the Synchrotron Radiation Center (SRC) in Stoughton, WI (USA). Both normal-incidence monochromators have, naturally, hardly any photon flux above 40 eV, so that second-order light does not pose a problem for energies above 22 eV. For the higher photon energies we employed the PGM beamline with an Al filter to suppress higher order light.

The Wadsworth beamline does not have an entrance slit and the exit slit was set at 200 μm that yielded a resolution of about 32 meV at 28.5 eV. The entrance and exit slits of the U1-NIM beamline were set at 250 μm that yielded a resolution of 11 meV at 28.5 eV. For both beamlines the Ar $3s \rightarrow 6p$ resonance has been used to determine the energy resolution as well as the energy offset of the beamline. The entrance and exit slits on the PGM beamline were set at 255 and 150 μm , respectively, providing a high photon flux with a resolution of 12 meV at 47 eV. The Ne $2s \rightarrow 4p$ resonance has been used for energy calibration of this beamline.

The photon beam enters through a differential pumping stage into the interaction region inside the vacuum chamber where it crosses a beam of Mg atoms produced by a resistively heated oven. The Mg is heated to a temperature of about 395 °C. The crucible is biased to +2 V in order to keep thermal electrons inside the oven, thus avoiding electron-impact ionization of Mg. A pulsed electric field accelerates the photoions toward a drift tube with a Z stack of microchannel plates (MCP) at its end. A more detailed description of the setup can be found elsewhere [32].

We extract the areas of the singly and doubly charged ion peaks of the main Mg isotope in our time-of-flight spectra using direct numerical integration. For some of the Mg spectra we have leaked neon into the chamber producing an additional Ne^+ peak in the spectrum, which we use to determine the relative Mg^+ cross section,

$$\sigma_{\text{rel}}(\text{Mg}^+) = \sigma(\text{Ne}^+) \frac{A(\text{Mg}^+)}{A(\text{Ne}^+)}. \quad (1)$$

Here, $\sigma(\text{Ne}^+)$ is the neon single photoionization cross section [33], and $A(\text{Mg}^+)$ and $A(\text{Ne}^+)$ are the areas of the Mg^+ and Ne^+ peaks in our spectra, respectively. This method assumes a constant Mg and Ne gas pressure but is insensitive to photon flux variations.

III. RESULTS AND DISCUSSION

Figure 1 shows our double-to-single photoionization cross section ratio from the threshold to 54 eV photon energy together with other data. We have also indicated in Fig. 1 the $2p_{3/2}$ and $2p_{1/2}$ thresholds for second-order light (photons with twice the desired photon energy) because second-order light can alter the double-to-single photoionization ratio significantly due to the onset of Auger decay around 55 eV. However, no appreciable effect due to second-order light is visible in the ratio.

The theoretical ratio obtained using the convergent close coupling (CCC) method [3] is depicted by red asterisks con-

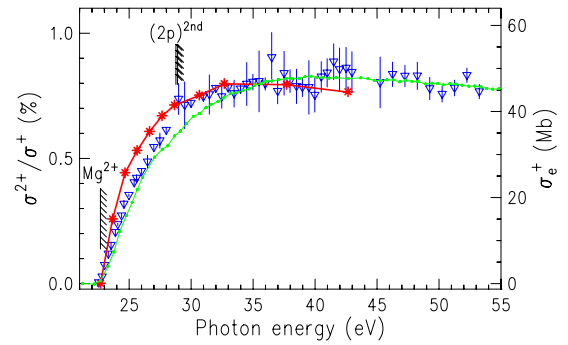


FIG. 1. (Color online) Double-to-single photoionization ratio of Mg as a function of photon energy. Triangles: this work; asterisks connected with a line: CCC theory [3]. The solid line with dots is the experimental electron-impact single-ionization cross section of Mg^+ [34] (cross section scale is on the right-hand side). The double-ionization threshold (Mg^{2+}) as well as the $2p$ thresholds for second-order light [$(2p)^{2\text{nd}}$] is indicated.

nected with a line to guide the eye. While there is a general agreement between theory and experiment, there is a distinct deviation at lower energies, namely, the theoretical ratio exhibits a much steeper rise and stays slightly above the experimental data. Above 29 eV the theoretical curve is within our error bars. The deviation of theory from experiment may be due to the frozen-core model used in the CCC calculation. While this approximation worked well in the case of Be, the first inner shell of Mg is much closer to the valence shell as compared to Be. Thus the Mg $2p$ inner shell has possibly a significant influence on the valence single and double photoionization cross section.

Also shown in Fig. 1 is the electron-impact single-ionization cross section for Mg^+ ions [34] for comparison with the double-to-single photoionization ratio of Mg. This comparison is based on a model introduced by Samson nearly 20 years ago [35] suggesting that both processes, double photoionization of an atom and electron-impact ionization of the corresponding ion, are similar in that they have the same final state: a doubly charged ion. The double-ionization process is thought of as a two-step process: In the first step one electron is photoionized, which, on its way out, kicks in the second step another electron into the continuum. The electron-impact cross section has indeed a similar energy dependence as our ratio but is slightly smaller at lower energies if one scales the electron-impact data to our ratio at high energies. This difference may be due to the energy-dependent shake-off process that contributes to the double-photoionization but not to the electron-impact cross section. Overall, the electron-impact data seem to be closer to our data than theory but show a less pronounced curvature. However, the electron-impact data have a free scaling parameter.

Previously, a scaling model for the double-to-single photoionization ratio has been introduced [4,27] and its applicability was later confirmed [36]. Briefly, this model allows us to accurately describe the energy dependence of the ratio for Li, Be, Na, and K based on the ratio curve for He [37], with the hope that this scaling model is applicable to all atoms as long as autoionization and Auger processes do not contribute to the double-ionization process. In order to apply

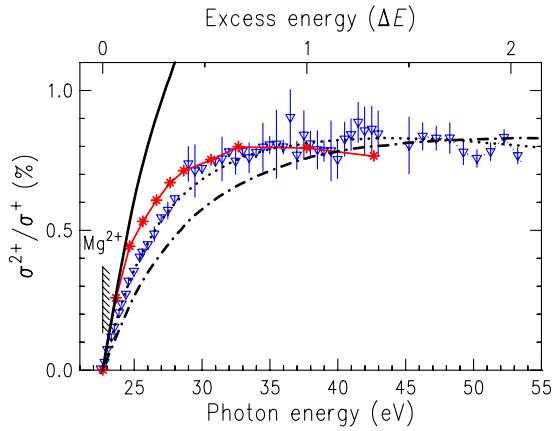


FIG. 2. (Color online) Double-to-single photoionization ratio of Mg as a function of photon energy. The axis on the top shows the excess energy in units of the ionization energy of the Mg^+ ion. Triangles: this work; asterisks connected with a line: CCC theory [3]. The different lines represent the results of a scaling model using different scaling factors (see text for details).

the scaling model the ratio curve of an atom has to be plotted on an energy scale in units of ΔE [4] with

$$\Delta E = E^{2+} - E^+, \quad (2)$$

where E^{2+} and E^+ are the ionization thresholds for double and single ionization, respectively. The energy ΔE is equivalent to the ionization potential of the corresponding ion. If the two electrons originate from two different shells, the ionization threshold of the more strongly bound electron is used, possibly because the stronger bond electron has typically a larger cross section. Moreover, the maximum nonresonant double-to-single photoionization ratio R_{\max} for a given double-ionization process can be expressed according to the scaling model [28] by

$$R_{\max} = c(\sqrt{E^{2+}} - \sqrt{E^+}), \quad (3)$$

where the constant $c \approx 0.01 \text{ eV}^{-0.5}$ and is assumed to be the same for all elements.

Note that, as mentioned above, autoionization and Auger decay processes are not included in this model. This means we have to restrict any test of the model to the energy region below the first inner-shell threshold that allows Auger decay. More information about the model can be found in Ref. [28].

In Fig. 2 we show again our double-to-single photoionization ratio along with the CCC calculation [3]. In addition, we show the ratio predicted by the scaling model as a solid line using the above equations for Mg. Surprisingly, the experimental ratio is much smaller than the one predicted by the model. Interestingly, there is some agreement of the model curve with the theoretical calculation insofar as the slope at threshold is very similar. Scaling the ratio of the model curve down so that the curve matches the experimental data at high energies results in the dashed-dotted line displayed in Fig. 2. This curve still does not fit our data and only an additional energy scaling (dotted line) leads to a satisfactory agreement with our measured ratio. In other words, while the double-to-single photoionization ratio curve of Mg exhibits the same

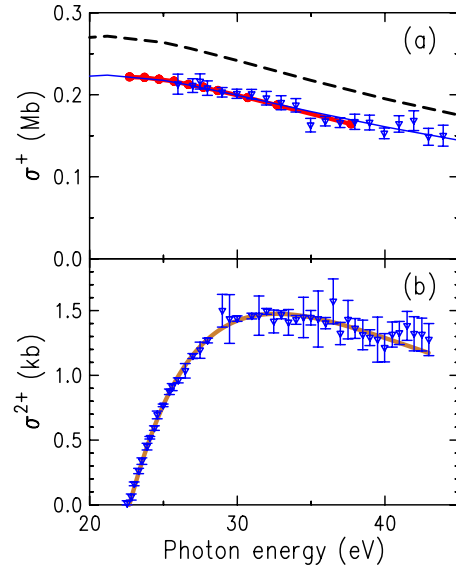


FIG. 3. (Color online) (a) Single photoionization cross section of Mg as a function of photon energy; triangles: this work; thin line: theoretical total cross section [38] scaled to fit our data. Thick line with circles: CCC theory [3]; dashed line: theoretical total cross section [38]. (b) Double-photoionization cross section of Mg as a function of photon energy; triangles: this work; solid line: shape function [39].

shape as the ratio curve for He, the scaling factors—necessary to scale the energy axis as well as the magnitude of the ratio—are not correctly predicted by the equations of the scaling model given above. We do not see any reason why the scaling model breaks down in the case of Mg as it was successfully applied in other cases.

As mentioned above, for some of the spectra we have leaked neon into the chamber in order to determine the relative Mg^+ cross section that is displayed in Fig. 3(a). Note that the error bars shown are only statistical error bars. When we scale the experimental relative cross sections to the theoretical Mg^+ cross section curve [3] (red circles connected with a solid line), we find good agreement between experiment and theory. The total cross section calculated by Yeh and Lindau [38] is too high but runs almost parallel to our data. In order to obtain a smooth cross section curve that represents our data in the entire region of interest we scale the total cross section curve [38] to fit our data (thin blue line). Even though the total cross section curve includes the Mg^{2+} cross section we obtain a well matching curve within our error bars.

Using the smooth curve for our Mg^+ cross section mentioned above and using our double-to-single photoionization ratio we determine the double-photoionization cross section displayed in Fig. 3(b). In the same panel we show a shape function that was developed by Pattard [39]. It models the energy dependence of our double-photoionization cross section very well although it is argued in the paper that this shape function works best for the *complete* break up, i.e., all target electrons are ionized. This shape function describes the transition between threshold behavior and high-energy behavior of the cross section and has two fit parameters, namely, the maximal cross section σ_M and the energy position of the maximum E_M .

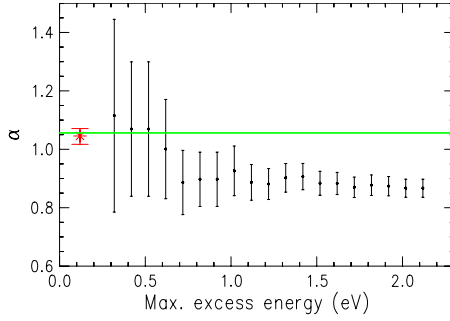


FIG. 4. (Color online) Wannier exponent α for different least-squares fits to our data from threshold to a chosen maximal excess energy. The asterisk with error bar represents the Wannier exponent derived from a shape-function fit using Eq. (4) and is plotted at an arbitrary energy position. The horizontal line indicates the theoretical Wannier exponent of 1.056.

$$\sigma(E) = \sigma_M x^\alpha \left(\frac{\alpha + 7/2}{\alpha x + 7/2} \right)^{\alpha+7/2}. \quad (4)$$

Here, α is the Wannier exponent and $x = E/E_M$ with $E = h\nu - E_{\text{thr}}$ the excess energy, $h\nu$ the photon energy, and E_{thr} the double-ionization threshold.

We took a closer look at the near-threshold double-photoionization cross section to examine the range of validity of Wannier's threshold law [25]. We performed least-squares fits to our data for different maximal excess energies with the lower limit of the fit range always at the threshold employing the following equation:

$$\sigma(h\nu - E_{\text{thr}}) = \sigma_0 (h\nu - E_{\text{thr}})^\alpha. \quad (5)$$

Here, $h\nu$ is the photon energy, E_{thr} the double-ionization threshold, σ_0 a proportionality constant corresponding to the cross section at 1 eV, and α the Wannier exponent. The fit results for the different fit ranges are displayed in Fig. 4 showing the Wannier exponent α as a function of the upper limit of the fit range. We determine the double-ionization threshold to be at 22.68(4) eV in very good agreement with the literature value of 22.681 515(13) eV [40]. Due to the small number of data points the error bars are rather large for the data very close to threshold, but it can be seen that the experimental Wannier exponent is in accord with the theoretical value of 1.056 (shown as a horizontal line in Fig. 4) close to threshold and is then decreasing to about 0.9 for excess energies above 0.7 eV. This range of validity is smaller than for He (ca. 2 eV) [41] and Be (ca. 1.7 eV) [5] but is similar to Li (ca. 0.7 eV) [42]. The proportionality constant σ_0 for Mg is 0.43(8) kb, which is clearly smaller than the ones for He [1.021(5) kb] [41], Li [3.32(3) kb] [42], and Be (2.6 kb) [5].

Looking for an alternative to the method described above, we employed the shape function [39] defined in Eq. (4) with α as a *free* fit parameter in order to derive the Wannier exponent. This procedure has the advantage that more data points can be included in the fit and not just a few very close

to threshold. From that fit using all data up to 39 eV we derive $\alpha = 1.044(27)$ in good agreement with the theoretical value of 1.056. This point is shown in Fig. 4 as an asterisk at an arbitrary energy position near threshold. In turn, the good agreement demonstrates that the threshold behavior has indeed “observable consequences for the shape of the respective cross section” as noted by Pattard [39].

Unfortunately, the large error bars for the double-photoionization cross section do not allow us to test the Coulomb-dipole theory [26] and small oscillations in the cross section can thus not be discerned.

IV. CONCLUSION

We have measured the relative single photoionization cross section and double-to-single photoionization ratio of Mg from the double-ionization threshold to 54 eV and derived the corresponding relative double-photoionization cross section. Our data allow us to make a detailed comparison with theory. We find qualitative agreement with the CCC calculations by Kheifets and Bray [3], but also notice that theory predicts a steeper slope near threshold resulting in too high a ratio below 29 eV. The discrepancy between theory and experiment is possibly due to the frozen-core approximation used in the calculation, which may not be strictly valid in the case of Mg. The electron-impact ionization cross section of Mg^+ exhibits a similar energy dependence as our double-to-single photoionization ratio and is slightly lower at lower energies when scaled to match our data at high energies. A previously introduced scaling model for the double-to-single photoionization ratio does not quantitatively fit our Mg data but with suitable scaling factors it can match the double-to-single photoionization ratio curve for He to the one for Mg.

The photon energy dependence of our relative Mg^+ cross section is in accord with a recently performed CCC calculation of the Mg^+ cross section [3]. A numerical shape function [39] can be applied successfully to our double-photoionization cross section curve.

We have applied Wannier's threshold law to our near-threshold Mg^{2+} data and find a rather short range of validity of ca. 0.7 eV with a cross section σ_0 that is clearly smaller than the one for He, Li, and Be.

ACKNOWLEDGMENTS

The authors wish to thank the staff of the Synchrotron Radiation Center for their excellent technical support. We also thank Dr. A. Kheifets for helpful discussions and for sending his data in numerical form. We are grateful to Dr. S. Whitfield for a critical reading of the manuscript. D.V.L. was partly supported by the Ministry of Science and Technological Development, Serbia. This work is based upon research conducted at the Synchrotron Radiation Center, University of Wisconsin-Madison, which is supported by the NSF under Grant No. DMR-0537588.

- [1] J. S. Briggs and V. Schmidt, *J. Phys. B* **33**, R1 (2000).
- [2] I. Bray, D. V. Fursa, A. S. Kheifets, and A. T. Stelbovics, *J. Phys. B* **35**, R117 (2002), and references therein.
- [3] A. S. Kheifets and I. Bray, *Phys. Rev. A* **75**, 042703 (2007).
- [4] R. Wehlitz and S. B. Whitfield, *J. Phys. B* **34**, L719 (2001).
- [5] D. Lukić, J. B. Bluett, and R. Wehlitz, *Phys. Rev. Lett.* **93**, 023003 (2004).
- [6] R. Wehlitz, D. Lukić, and J. B. Bluett, *Phys. Rev. A* **71**, 012707 (2005).
- [7] S. Hasegawa, F. Yoshida, L. Matsuoka, F. Koike, S. Fritzsche, S. Obara, Y. Azuma, and T. Nagata, *Phys. Rev. Lett.* **97**, 023001 (2006).
- [8] F. Yoshida, L. Matsuoka, R. Takashima, T. Nagata, Y. Azuma, S. Obara, F. Koike, and S. Hasegawa, *Phys. Rev. A* **73**, 062709 (2006).
- [9] K. Berrington, J. Pelan, and L. Quigley, *J. Phys. B* **30**, 4973 (1997).
- [10] A. S. Kheifets and I. Bray, *Phys. Rev. A* **65**, 012710 (2001).
- [11] J. Colgan and M. S. Pindzola, *Phys. Rev. A* **65**, 022709 (2002).
- [12] J. Colgan, M. S. Pindzola, and F. Robicheaux, *Phys. Rev. A* **72**, 022727 (2005).
- [13] F. Citrini, L. Malegat, P. Selles, and A. K. Kazansky, *Phys. Rev. A* **67**, 042709 (2003).
- [14] A. K. Kazansky and V. N. Ostrovsky, *J. Phys. B* **30**, L835 (1997).
- [15] Y. Sato, T. Hayaishi, Y. Itikawa, Y. Itoh, J. Murakami, T. Nagata, B. Sonntag, A. Yagishita, and M. Yoshino, *J. Phys. B* **18**, 225 (1985).
- [16] K. J. Ross, J. B. West, H.-J. Beyer, and A. De Fanis, *J. Phys. B* **32**, 2927 (1999).
- [17] H.-J. Beyer, J. B. West, K. J. Ross, and A. De Fanis, *J. Phys. B* **33**, L767 (2000).
- [18] F. Maulbetsch, I. L. Cooper, and A. S. Dickinson, *J. Phys. B* **33**, L119 (2000).
- [19] L. Malegat, F. Citrini, P. Selles, and P. Archirel, *J. Phys. B* **33**, 2409 (2000).
- [20] J. B. West, K. J. Ross, H.-J. Beyer, A. De Fanis, and H. Hamdy, *J. Phys. B* **34**, 4169 (2001).
- [21] A. De Fanis, H.-J. Beyer, K. J. Ross, and J. B. West, *J. Phys. B* **34**, L99 (2001).
- [22] D. M. P. Holland and K. Codling, *J. Phys. B* **13**, L293 (1980).
- [23] D. M. P. Holland, K. Codling, and R. N. Chamberlain, *J. Phys. B* **14**, 839 (1981).
- [24] T. Nagata, Y. Itoh, T. Hayaishi, Y. Itikawa, T. Koizumi, T. Matsuo, Y. Sato, E. Shigemasa, A. Yagishita, and M. Yoshino, *J. Phys. B* **22**, 3865 (1989).
- [25] G. H. Wannier, *Phys. Rev.* **90**, 817 (1953).
- [26] A. Temkin and A. K. Bhatia, *Bull. Am. Phys. Soc.* **53**, 38 (2008).
- [27] R. Wehlitz, J. B. Bluett, and S. B. Whitfield, *Phys. Rev. A* **66**, 012701 (2002).
- [28] J. B. Bluett, D. Lukić, S. B. Whitfield, and R. Wehlitz, *Nucl. Instrum. Methods Phys. Res. B* **241**, 114 (2005).
- [29] J. Bisognano, M. Severson, M. A. Green, G. Rogers, M. Fisher, T. Kubala, and M. Bissen, *Nucl. Instrum. Methods Phys. Res. A* **467**, 492 (2001).
- [30] T. Kubala, M. Bissen, M. Severson, G. Rogers, D. Wallace, M. Thikim, and M. V. Fisher, in *Proceedings of the SRI: Eleventh US National Conference*, edited by P. Pianetta, J. Arthur, and S. Brennan, AIP Conf. Proc. No. 521 (AIP, New York, 2000), p. 91.
- [31] R. Reininger, S. L. Crossley, M. A. Lagergren, M. C. Severson, and R. W. C. Hansen, *Nucl. Instrum. Methods Phys. Res. A* **347**, 304 (1994).
- [32] R. Wehlitz, D. Lukić, C. Koncz, and I. A. Sellin, *Rev. Sci. Instrum.* **73**, 1671 (2002).
- [33] J. M. Bizau and F. J. Wuilleumier, *J. Electron Spectrosc. Relat. Phenom.* **71**, 205 (1995).
- [34] B. Peart, J. W. G. Thomason, and K. Dolder, *J. Phys. B* **24**, 4453 (1991).
- [35] J. A. R. Samson, *Phys. Rev. Lett.* **65**, 2861 (1990).
- [36] P. N. Juranić, J. Nordberg, and R. Wehlitz, *Phys. Rev. A* **74**, 042707 (2006).
- [37] J. A. R. Samson, W. C. Stolte, Z. X. He, J. N. Cutler, Y. Lu, and R. J. Bartlett, *Phys. Rev. A* **57**, 1906 (1998).
- [38] J. J. Yeh and I. Lindau, *At. Data Nucl. Data Tables* **32**, 1 (1985).
- [39] T. Pattard, *J. Phys. B* **35**, L207 (2002).
- [40] V. Kaufman and W. C. Martin, *J. Phys. Chem. Ref. Data* **20**, 83 (1990).
- [41] H. Kossmann, V. Schmidt, and T. Andersen, *Phys. Rev. Lett.* **60**, 1266 (1988).
- [42] R. Wehlitz, J. B. Bluett, and S. B. Whitfield, *Phys. Rev. Lett.* **89**, 093002 (2002).